d-wave superconductivity in twisted bilayer graphene: a phonon mechanism

Fengcheng Wu

University of Maryland

- F. Wu, A. H. MacDonald and I. Martin, Phys. Rev. Lett. **121**, 257001 (2018).
- F. Wu, arXiv:1811.10620

Outline

1. Phonon-mediated superconductivity in tBLG [PRL 121, 257001 (2018)]

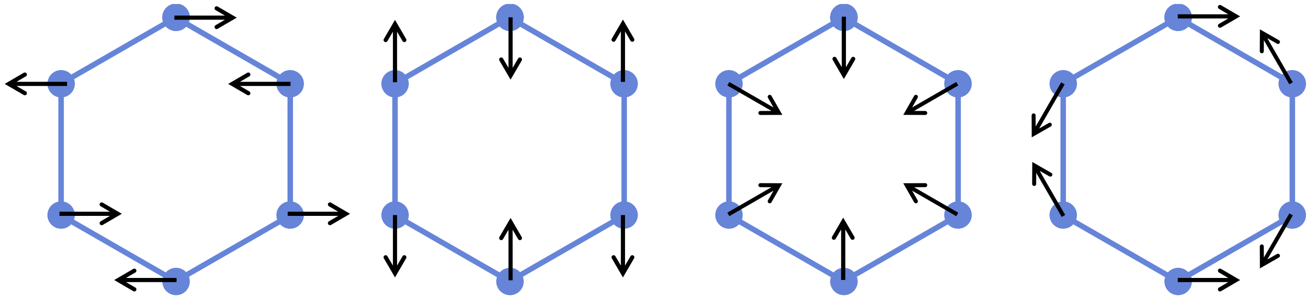

(a) $E_2, \hat{u}_x$ (b) $E_2, \hat{u}_y$ (c) $A_1, \hat{u}_a$ (d) $B_1, \hat{u}_b$

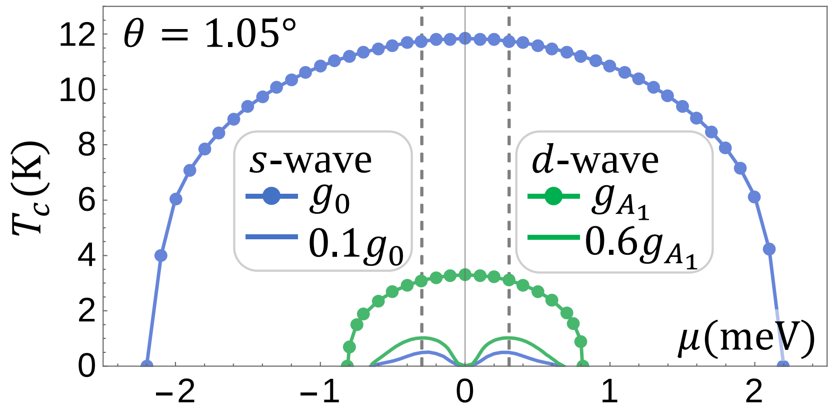

- Phonons generate attractive interaction in both *s* and *d* wave pairing channels.
- The attraction combined with band flattening leads to observable T_c.

2. Chiral *d*-wave state [arXiv:1811.10620]

- Gap structure, topological character
- Spontaneous vortices, spontaneous supercurrent

3. Strain & In-plane magnetic field [in progress, to appear (arXiv:1904.07875)]

- Both stabilize nematic d-wave state

Experiments

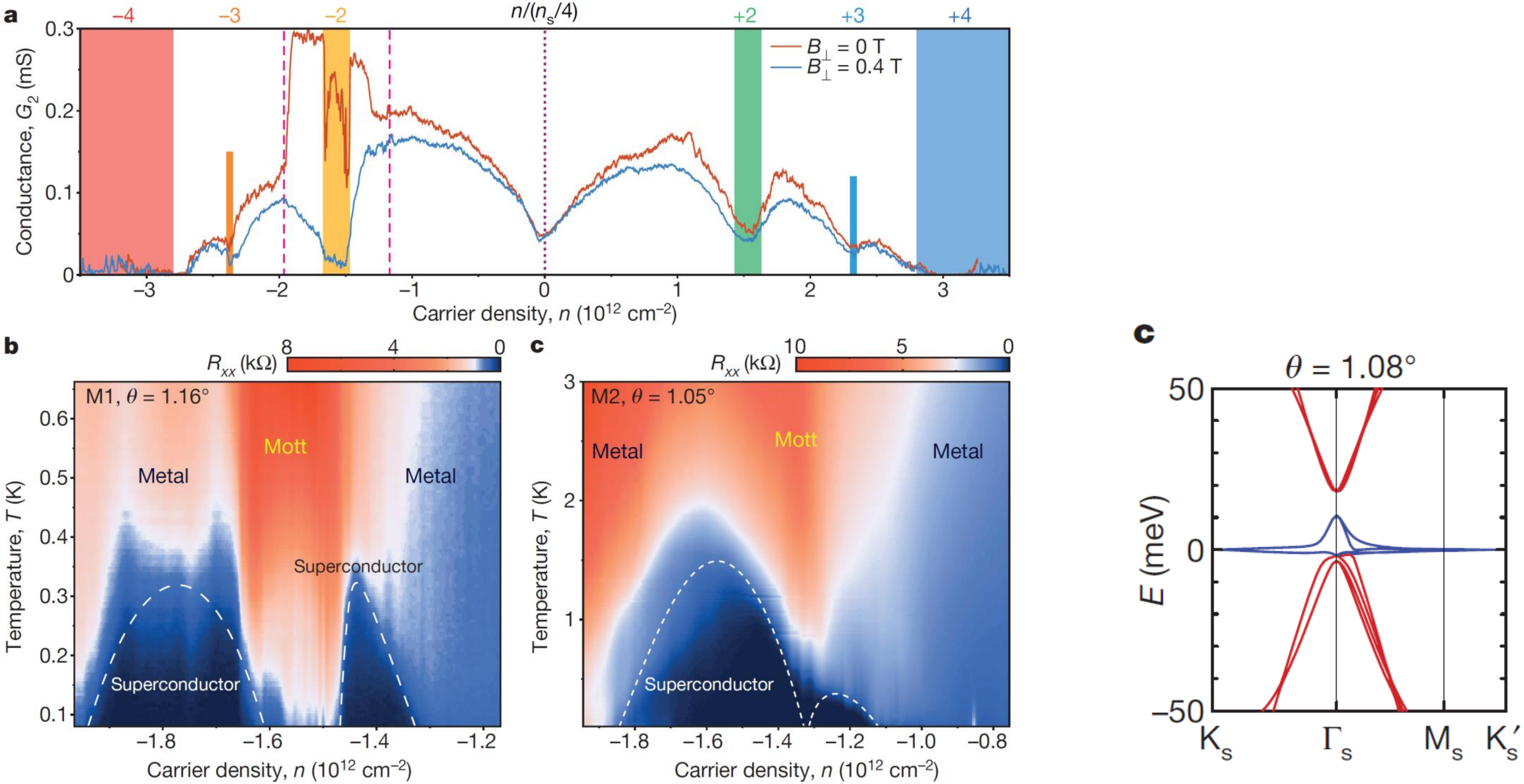

Y. Cao, *et al.*, Nature 556, 80 (2018), Nature 556, 43 (2018)

M. Yankowitz, *et al.*, arXiv:1808.07865

Assumption

- Assumption: Correlated insulators and superconductors are competing states.

- Correlated insulators:
  - Ferromagnetism with flavor polarization (spin, valley, sublattice, layer)?
  - Density wave (charge/spin/valley)?
  - ……

- SC could be simpler:
  - ✓ Inter-valley pairing
  - ✓ Spin SU(2) symmetry:

    (1) spin singlet pairing, *s*-wave, *d*-wave

    (2) spin triplet pairing, *p*-wave, *f*-wave

- A model pairing Hamiltonian derived from *e-ph* interaction
- Coulomb repulsion treated in a phenomenological way

Monolayer graphene

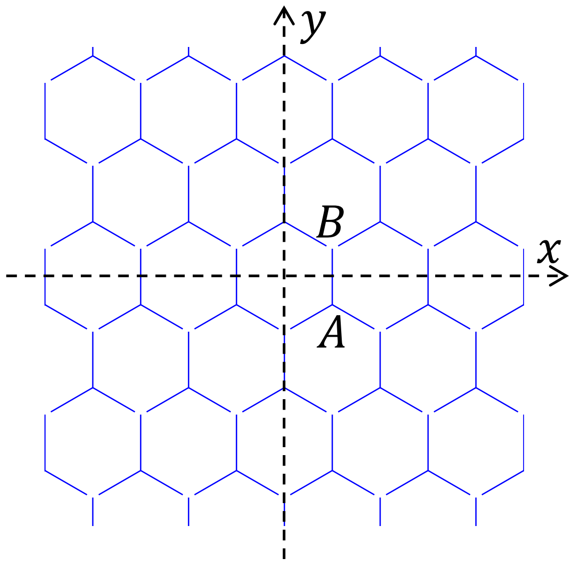

Honeycomb lattice

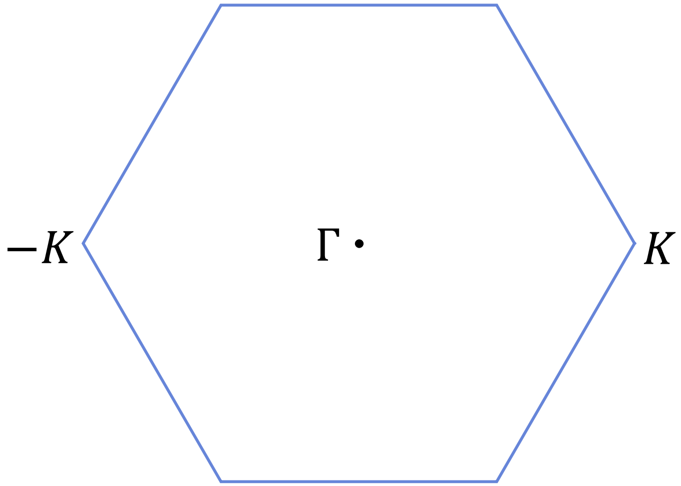

Brillouin zone

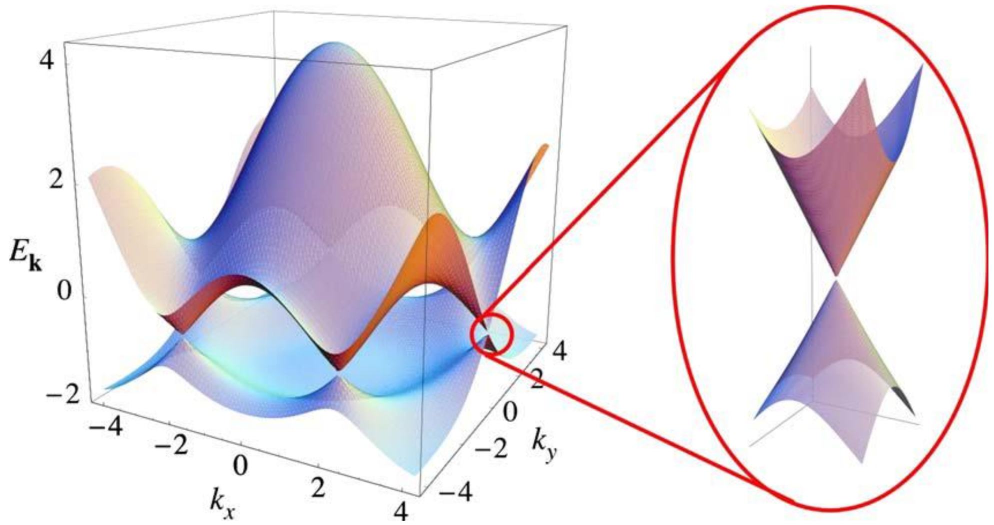

Dirac cone

- D_{6h} point group symmetry: $\hat{C}_{6z}, \hat{C}_{2x}, \hat{C}_{2y}, \widehat{M}_z$.
  spin SU(2) symmetry.

- Dirac cones at $\pm K$ valleys.
  At K valley, Dirac Hamiltonian: $\hbar v_F \boldsymbol{k}\cdot\boldsymbol{\sigma}$.

- $\hat{C}_{2z}\hat{T}$ protects the Dirac band touching.

- Sublattice pseudospin chirality

$$\hat{C}_{3z} c^{+}_{KA} \hat{C}^{-1}_{3z} = \exp(+i2\pi/3) c^{+}_{KA},$$
$$\hat{C}_{3z} c^{+}_{KB} \hat{C}^{-1}_{3z} = \exp(-i2\pi/3) c^{+}_{KB}$$

$$\hat{C}_{3z} c^{+}_{(-K)A} \hat{C}^{-1}_{3z} = \exp(-i2\pi/3) c^{+}_{(-K)A},$$
$$\hat{C}_{3z} c^{+}_{(-K)B} \hat{C}^{-1}_{3z} = \exp(+i2\pi/3) c^{+}_{(-K)B}$$

Twisted bilayer graphene

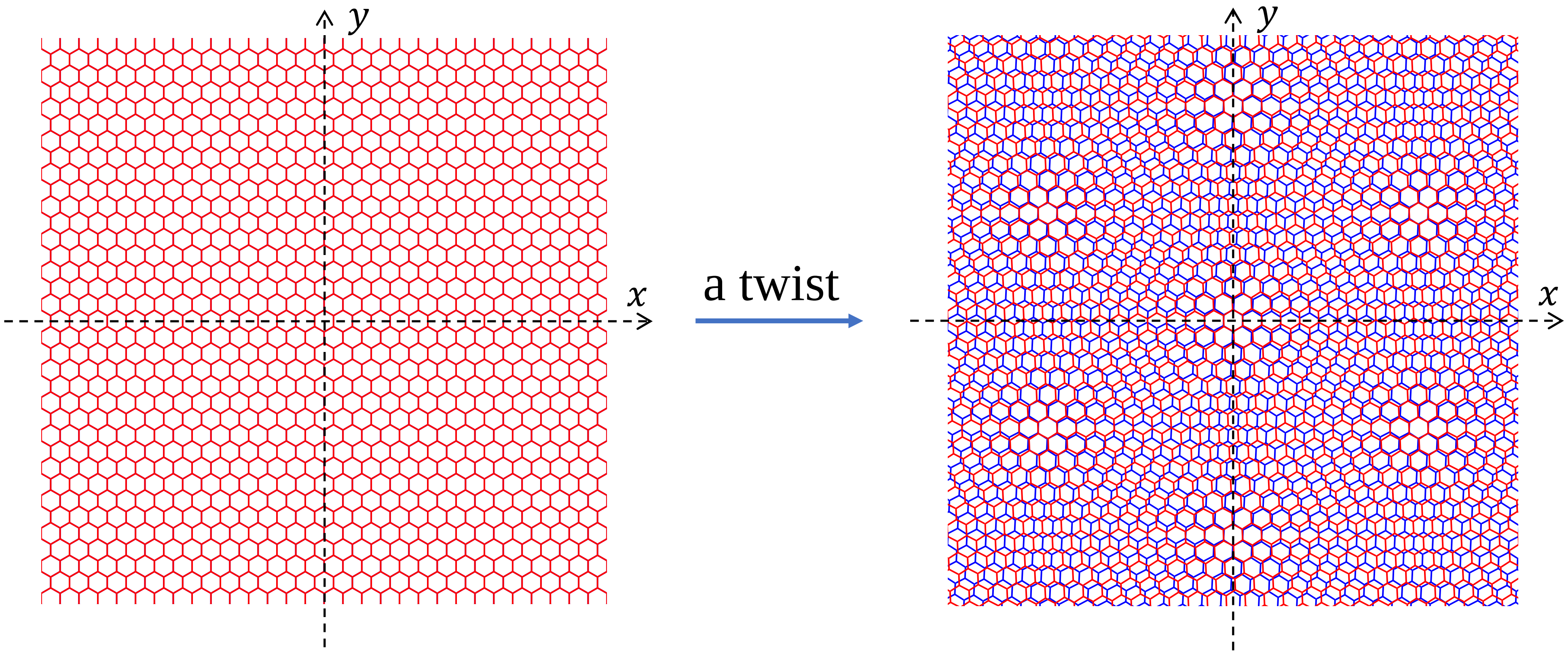

- D_6 point group symmetry: $\hat{C}_{6z}, \hat{C}_{2x}, \hat{C}_{2y}$.
- spin SU(2) symmetry
- Time-reversal symmetry
- valley U(1) symmetry

Moiré Hamiltonian

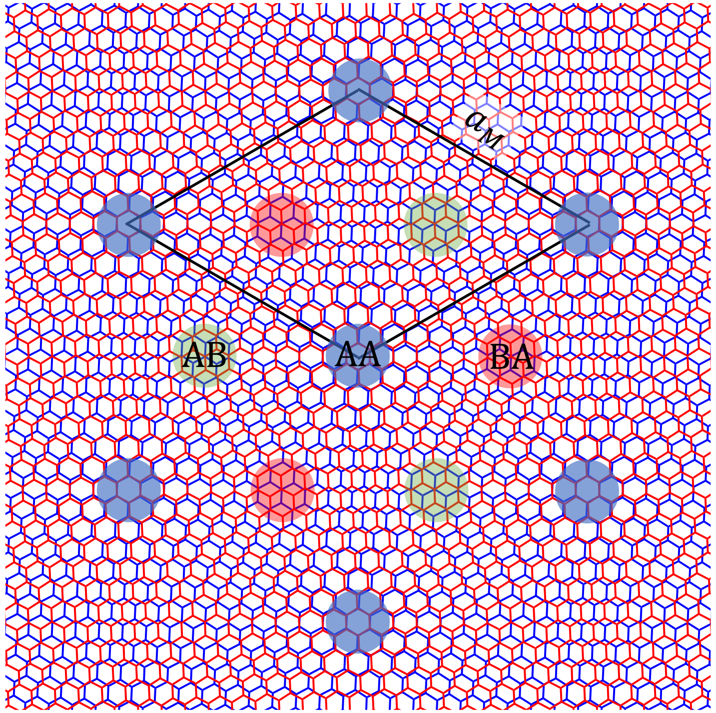

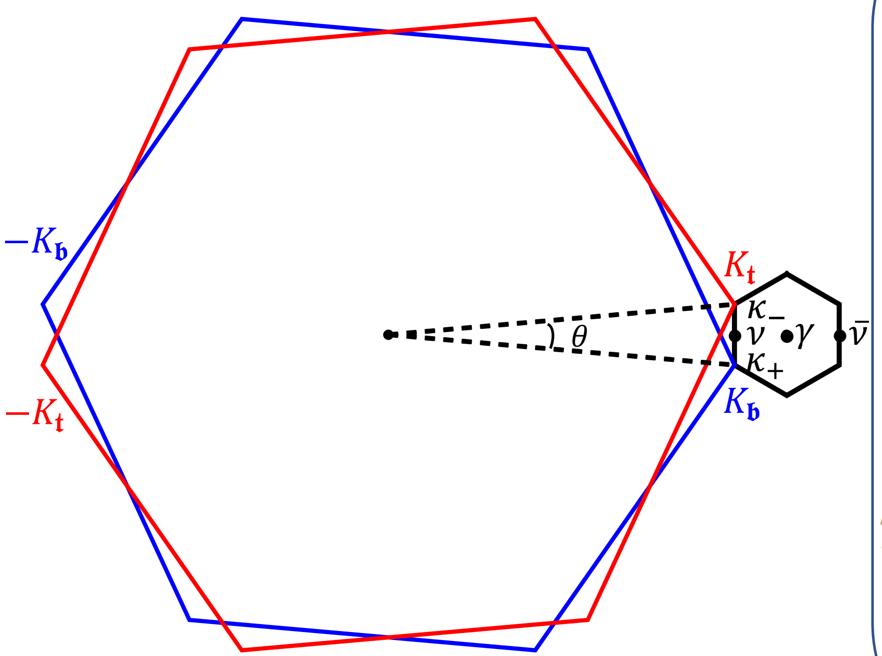

Moiré Hamiltonian in $+K$ valley:

$$\mathcal{H}_+ = \begin{pmatrix} h_\mathfrak{b}(\boldsymbol{k}) & T(\boldsymbol{r}) \\ T^\dagger(\boldsymbol{r}) & h_\mathfrak{t}(\boldsymbol{k}) \end{pmatrix}$$

- Dirac Hamiltonian

$$h_\ell(\boldsymbol{k}) = e^{-i\ell\frac{\theta}{4}\sigma_z}[\hbar v_F(\boldsymbol{k}-\boldsymbol{\kappa}_\ell)\cdot\boldsymbol{\sigma}]e^{+i\ell\frac{\theta}{4}\sigma_z}$$

- Interlayer tunneling

$$T(\boldsymbol{r}) = w\left[T_0 + e^{-i\boldsymbol{b}_+\cdot\boldsymbol{r}}T_{+1} + e^{-i\boldsymbol{b}_-\cdot\boldsymbol{r}}T_{-1}\right]$$

$$T_j = \begin{pmatrix} 1 & e^{-i2\pi j/3} \\ e^{i2\pi j/3} & 1 \end{pmatrix}$$

- Moiré pattern, period $a_M \approx a_0/\theta$
- Interlayer tunneling varies periodically.

J.M.B.L. dos Santos,et al, PRL (2007).
R. Bistritzer and A. H. MacDonald, PNAS

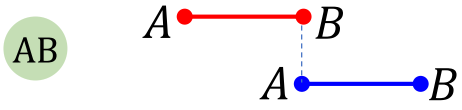

$$T\left(\boldsymbol{r} = -\frac{a_M}{\sqrt{3}}\hat{x}\right) = 3w\begin{pmatrix} 0 & 1 \\ 0 & 0 \end{pmatrix}$$

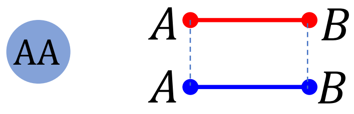

$$T(\boldsymbol{r} = 0) = 3w\begin{pmatrix} 1 & 0 \\ 0 & 1 \end{pmatrix}$$

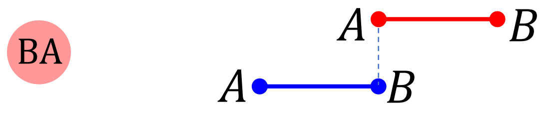

$$T\left(\boldsymbol{r} = \frac{a_M}{\sqrt{3}}\hat{x}\right) = 3w\begin{pmatrix} 0 & 0 \\ 1 & 0 \end{pmatrix}$$

Moiré band structure

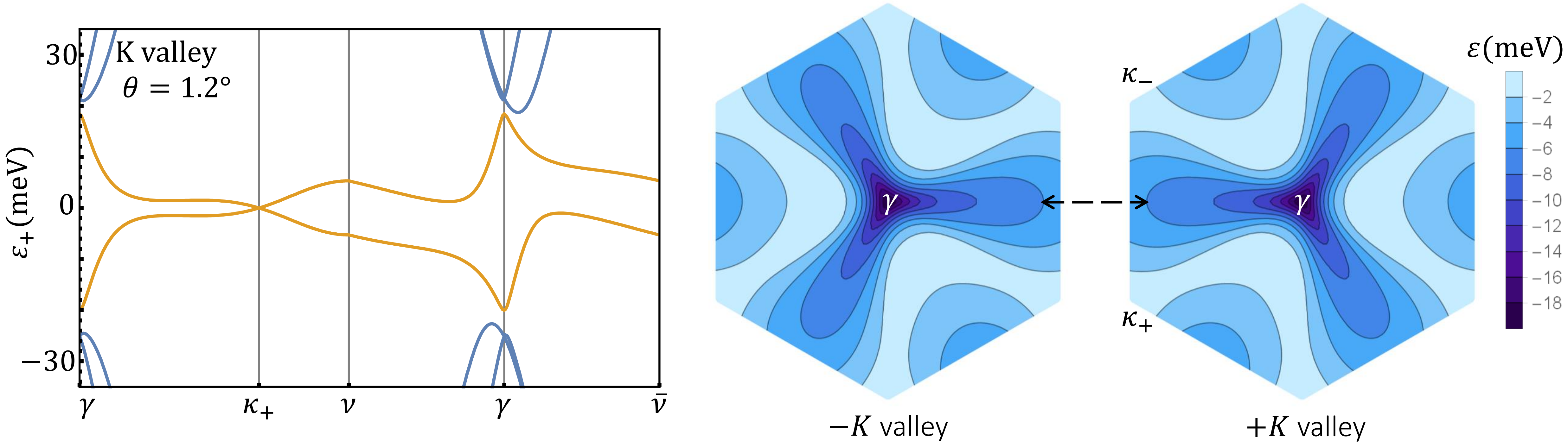

- $\hat{C}_{2z}\hat{T}$ protects the Dirac band touching.
- $\hat{C}_{3z}$ symmetry pins the Dirac point to $\boldsymbol{\kappa}_\pm$
- Band structure within one valley is "inversion" asymmetric

$$\varepsilon_\tau(\boldsymbol{q}) \neq \varepsilon_\tau(-\boldsymbol{q})$$

- Time-reversal symmetry connects the two valleys

$$\varepsilon_\tau(\boldsymbol{q}) = \varepsilon_{-\tau}(-\boldsymbol{q})$$

- Inter-valley pairing is more favored

Magic angle

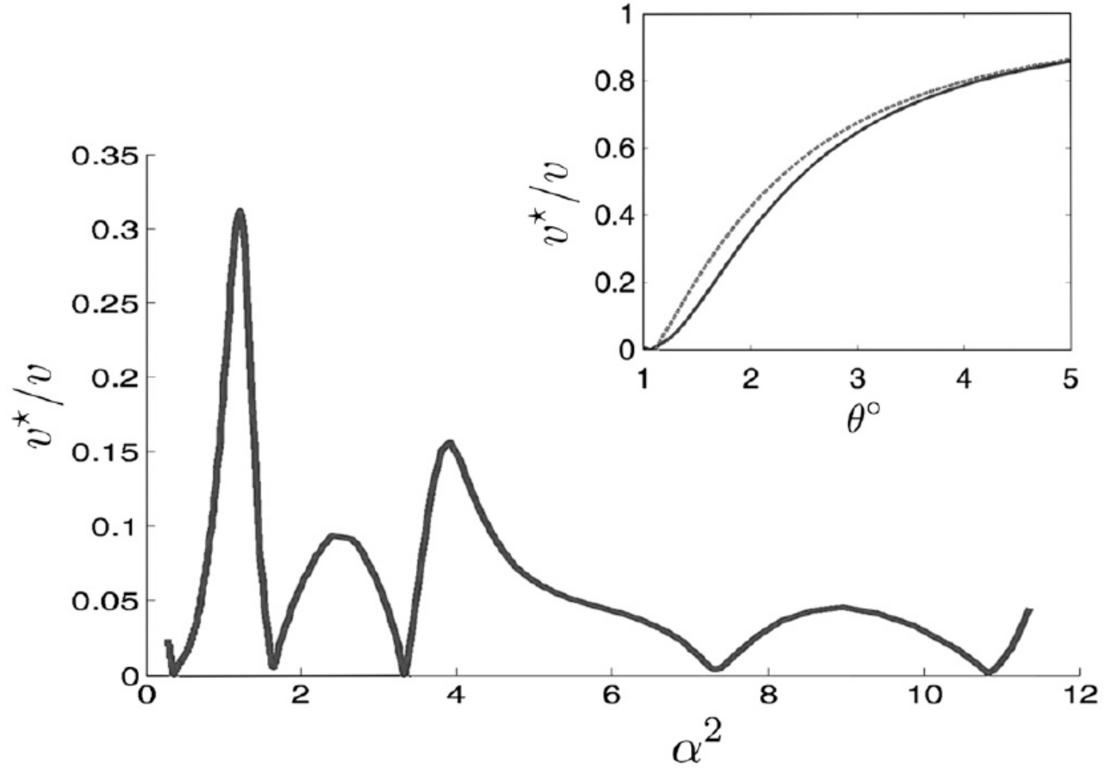

R. Bistritzer and A. H. MacDonald, PNAS 108, 12233 (2011).

$$\alpha = \frac{w}{\hbar v_F(\frac{4\pi}{3a_M})} = \frac{w}{\hbar v_F\,(\frac{4\pi}{3a_0})}\frac{1}{\theta}$$

- The Dirac velocity decreases to nearly zero around the magic angle.
- DOS is greatly enhanced ➔ interaction driven phase transitions.

Electron-Phonon Interaction

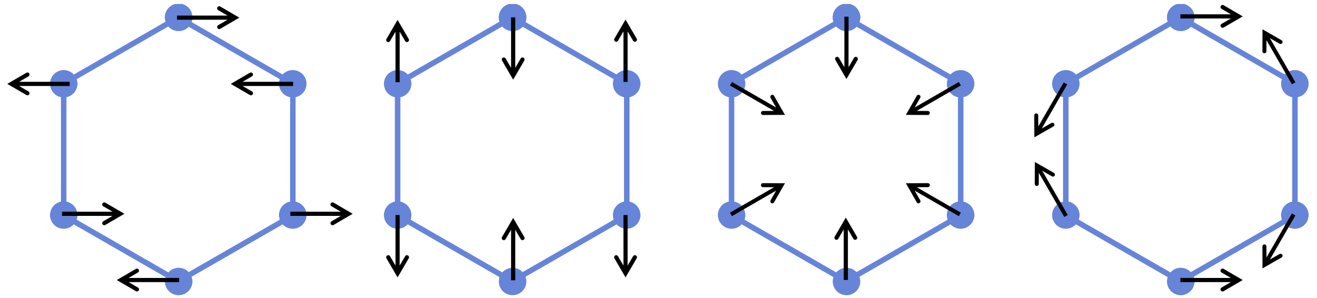

(a) $E_2, \hat{u}_x$ (b) $E_2, \hat{u}_y$ (c) $A_1, \hat{u}_a$ (d) $B_1, \hat{u}_b$

Γ phonons, 0.196 eV

$\pm K$ phonons, 0.17 eV

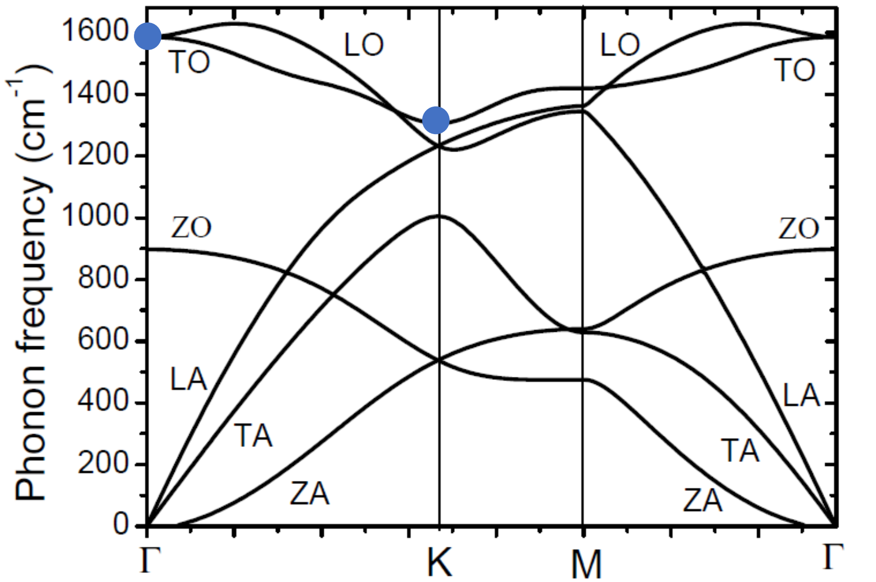

Phonon spectrum of monolayer graphene

- 4 optical phonon modes with in-plane atomic displacement.
- *e-ph* coupling:

$$H_{\mathrm{EPC}} = \int d^2\boldsymbol{r}\hat{\psi}^\dagger(\boldsymbol{r})\{F_{E_2}[\hat{u}_x(\boldsymbol{r})\tau_z\sigma_y - \hat{u}_y(\boldsymbol{r})\sigma_x] + F_{A_1}[\hat{u}_a(\boldsymbol{r})\tau_x\sigma_x + \hat{u}_b(\boldsymbol{r})\tau_y\sigma_x]\}\hat{\psi}(\boldsymbol{r})$$

Intra-valley scattering Inter-valley scattering

- Coupling strength:

$$F_{E_2} = F_{A_1} = \frac{3}{\sqrt{2}}\frac{\partial t_0}{\partial a_{CC}} = -3\beta\sqrt{\frac{3}{2}}\frac{\tilde{t}_0}{a_0}$$

t_0 is the nearest neighbor hopping parameter.

Phonon-mediated attraction

- *e-ph* coupling:

$$H_{\mathrm{EPC}} = \int d^2\boldsymbol{r}\hat{\psi}^\dagger(\boldsymbol{r})\{F_{E_2}[\hat{u}_x(\boldsymbol{r})\tau_z\sigma_y - \hat{u}_y(\boldsymbol{r})\sigma_x] + F_{A_1}[\hat{u}_a(\boldsymbol{r})\tau_x\sigma_x + \hat{u}_b(\boldsymbol{r})\tau_y\sigma_x]\}\hat{\psi}(\boldsymbol{r})$$

- Phonon quantization:

$$\hat{u}_\alpha(\boldsymbol{r}) = \sqrt{\frac{\hbar}{2NM\omega_\alpha}}\sum_{\boldsymbol{q}} e^{i\boldsymbol{q}\cdot\boldsymbol{r}}[a_\alpha(\boldsymbol{q}) + a_\alpha^\dagger(-\boldsymbol{q})]$$

Neglect $\boldsymbol{q}$ dependence of ω_α

- Phonon-mediated local attraction:

$$H_{\mathrm{att}} = -\int d^2\boldsymbol{r}\{g_{E_2}[(\hat{\psi}^\dagger\tau_z\sigma_y\hat{\psi})^2 + (\hat{\psi}^\dagger\sigma_x\hat{\psi})^2] + g_{A_1}[(\hat{\psi}^\dagger\tau_x\sigma_x\hat{\psi})^2 + (\hat{\psi}^\dagger\tau_y\sigma_x\hat{\psi})^2]\}.$$

- Attractive interaction strength:

$$g_\alpha = \frac{\mathcal{A}}{N}\left(\frac{F_\alpha}{\hbar\omega_\alpha}\right)^2\frac{\hbar^2}{2M} = \frac{27\sqrt{3}}{4}\beta^2\left(\frac{t_0}{\hbar\omega_\alpha}\right)^2\frac{\hbar^2}{2M}$$

$$g_{E_2} = 52\ \mathrm{meV\ nm}^2,\ g_{A_1} = 69\ \mathrm{meV\ nm}^2$$

BCS channel

- Phonon-mediated local attractive interaction:

$$H_{\rm att} = -\int d^2\boldsymbol{r}\{g_{E_2}[(\hat{\psi}^\dagger\tau_z\sigma_y\hat{\psi})^2 + (\hat{\psi}^\dagger\sigma_x\hat{\psi})^2] + g_{A_1}[(\hat{\psi}^\dagger\tau_x\sigma_x\hat{\psi})^2 + (\hat{\psi}^\dagger\tau_y\sigma_x\hat{\psi})^2]\}.$$

- Inter-valley pairing BCS channel:

$$\begin{aligned} H_{\rm BCS} = -4\int d^2\boldsymbol{r}\{ & g_{E_2}[\hat{\psi}^\dagger_{+As}\hat{\psi}^\dagger_{-As'}\hat{\psi}_{-Bs'}\hat{\psi}_{+Bs} + h.c.] \\ & + g_{A_1}[\hat{\psi}^\dagger_{+As}\hat{\psi}^\dagger_{-As'}\hat{\psi}_{+Bs'}\hat{\psi}_{-Bs} + h.c.] \\ & + g_{A_1}[\hat{\psi}^\dagger_{+As}\hat{\psi}^\dagger_{-Bs'}\hat{\psi}_{+As'}\hat{\psi}_{-Bs} + (A \leftrightarrow B)]\}, \end{aligned}$$

Intra-sublattice spin-singlet pairing: *s*-wave (first two terms)

Inter-sublattice spin-singlet pairing: *d*-wave (last term)

- electrons at different sublattices and opposite valleys have the same angular momentum under the three-fold rotation : $\hat{C}_{3z}\psi^+(\boldsymbol{r})\hat{C}_{3z}^{-1} = e^{i2\pi\tau_z\sigma_z/3}\psi^+(R_3\boldsymbol{r})$

Inter-valley Intra-sublattice pairing: *s*-wave

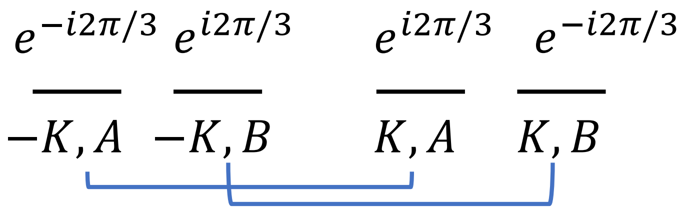

Inter-valley Inter-sublattice pairing: *d*-wave

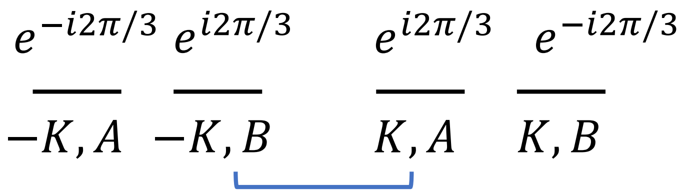

s-wave pairing

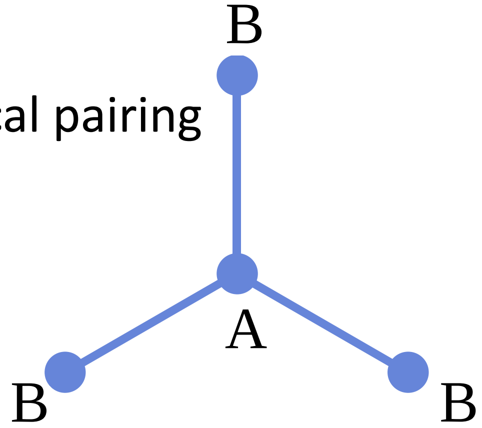

- Pair potential for intra-sublattice pairing

$$\Delta_\ell^{(s)}(\boldsymbol{r}) = \langle \hat{\psi}_{-\sigma\ell\downarrow}(\boldsymbol{r})\hat{\psi}_{+\sigma\ell\uparrow}(\boldsymbol{r})\rangle = -\langle \hat{\psi}_{-\sigma\ell\uparrow}(\boldsymbol{r})\hat{\psi}_{+\sigma\ell\downarrow}(\boldsymbol{r})\rangle$$

Spin singlet pairing

- Pair potential varies with the moiré period; Harmonics expansion with moiré reciprocal lattice vectors

$$\Delta_\ell^{(s)}(\boldsymbol{r}) = \sum_{\boldsymbol{b}} e^{i\boldsymbol{b}\cdot\boldsymbol{r}}\Delta_{\boldsymbol{b},\ell}^{(s)}$$

- Linearized gap equation:

$$\Delta_{\boldsymbol{b},\ell}^{(s)} = \sum_{\boldsymbol{b}'\ell'} \chi_{\boldsymbol{b}\boldsymbol{b}'}^{\ell\ell'} \Delta_{\boldsymbol{b}',\ell'}^{(s)},$$

$$\chi_{\boldsymbol{b}\boldsymbol{b}'}^{\ell\ell'} = \frac{2g_0}{\mathcal{A}} \sum_{\boldsymbol{q},n_1,n_2} \left\{ \frac{1-n_F[\varepsilon_{n_1}(\boldsymbol{q})]-n_F[\varepsilon_{n_2}(\boldsymbol{q})]}{\varepsilon_{n_1}(\boldsymbol{q})+\varepsilon_{n_2}(\boldsymbol{q})-2\mu} [\langle u_{n_1}(\boldsymbol{q})|u_{n_2}(\boldsymbol{q})\rangle_{\boldsymbol{b},\ell}]^* \langle u_{n_1}(\boldsymbol{q})|u_{n_2}(\boldsymbol{q})\rangle_{\boldsymbol{b}',\ell'} \right\}$$

$$g_0 = g_{E_2+}g_{A_1} = 121 \text{ meV nm}^2$$

$$\chi_{00} = g_0 \int d\varepsilon D(\varepsilon) \frac{1-2n_F(\varepsilon)}{2(\varepsilon-\mu)}$$

Dimensionless coupling constant is $g_0 D(\mu)$.

s-wave pairing

Near magic angle, $D(\mu)$ is of order 10 eV^{-1} nm^{-2} , and the dimensionless coupling constant $g_0 D(\mu) \sim 1$

➔ strong attractive interaction strength

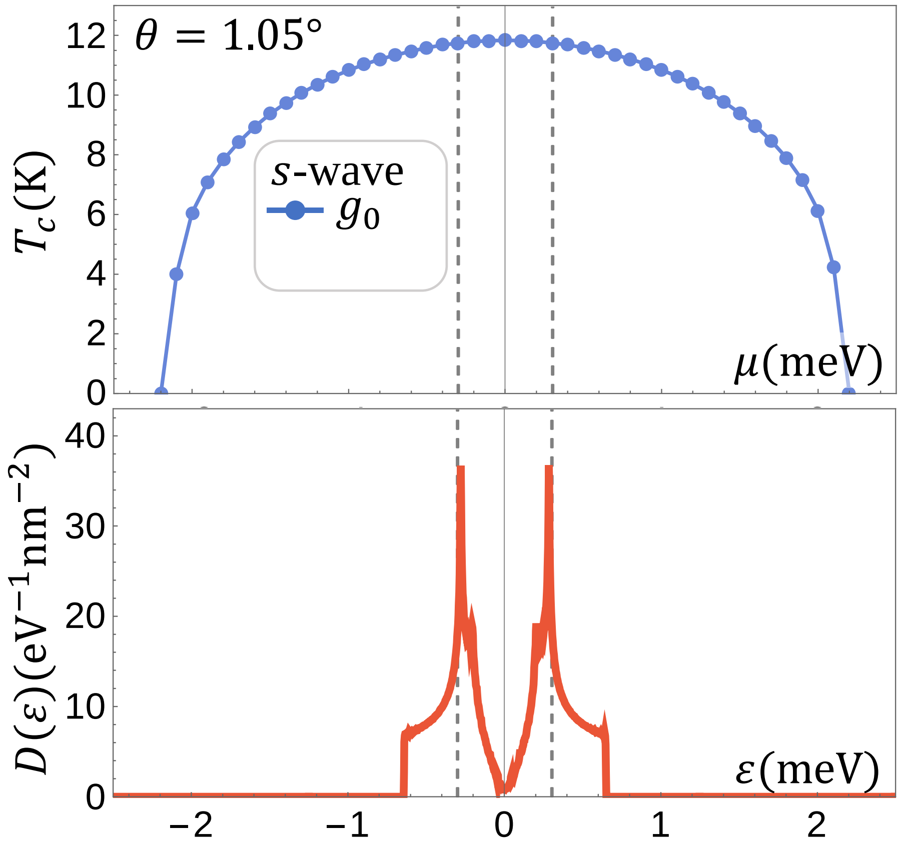

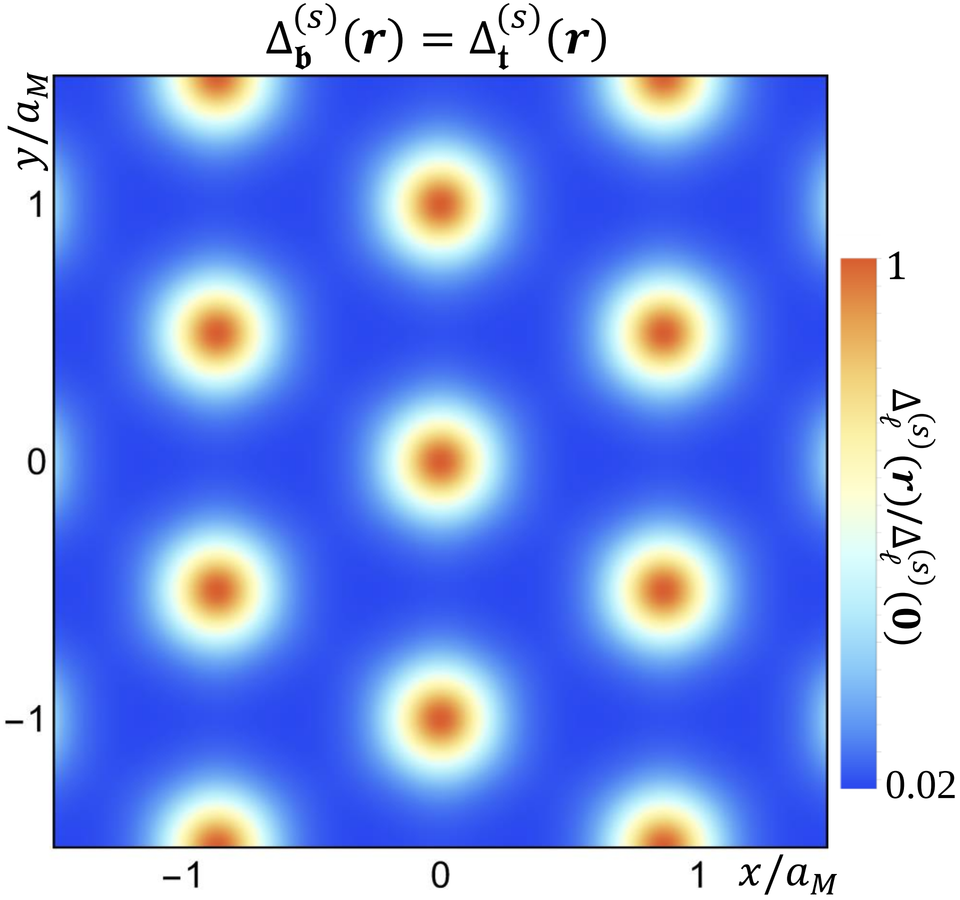

- $T_c \sim 10$ K .
- The pair amplitude modulates with the moiré period.

d-wave pairing

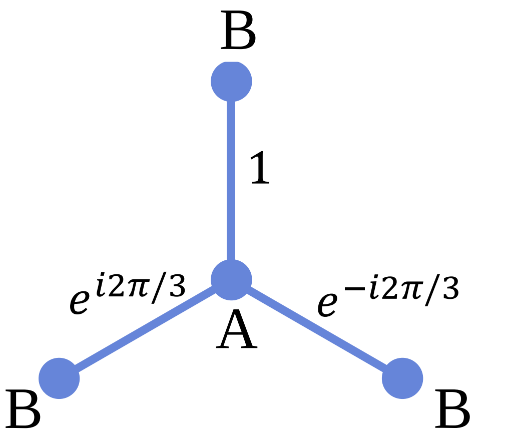

nearest-neighbor pairing

d_+: $\epsilon_{ss'}\hat{\psi}^\dagger_{+As}\hat{\psi}^\dagger_{-Bs'}$

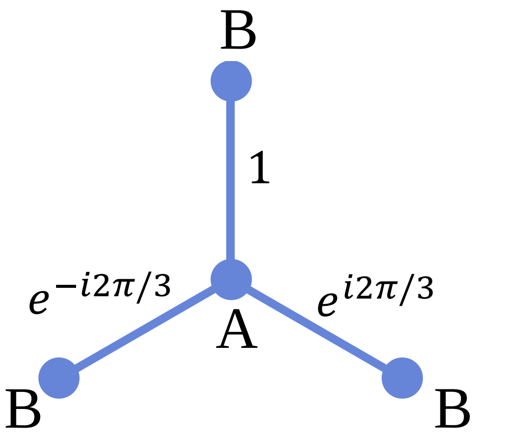

nearest-neighbor pairing

d_-: $\epsilon_{ss'}\hat{\psi}^\dagger_{+Bs}\hat{\psi}^\dagger_{-As'}$

- Chiral d-wave
- d_+-wave susceptibility:

$$\chi^{\ell\ell'}_{\boldsymbol{bb}} = \frac{4g_{A_1}}{\mathcal{A}} \sum_{\boldsymbol{q},n_1,n_2} \left\{ \frac{1 - n_F[\varepsilon_{n_1}(\boldsymbol{q})] - n_F[\varepsilon_{n_2}(\boldsymbol{q})]}{\varepsilon_{n_1}(\boldsymbol{q}) + \varepsilon_{n_2}(\boldsymbol{q}) - 2\mu} [\langle u_{n_1}(\boldsymbol{q})| \sigma_+ |u_{n_2}(\boldsymbol{q})\rangle_{\boldsymbol{b},\ell}]^* \langle u_{n_1}(\boldsymbol{q})| \sigma_+ |u_{n_2}(\boldsymbol{q})\rangle_{\boldsymbol{b}',\ell'} \right\}$$

- $\sigma_+ = \sigma_x + i\sigma_y$, closely related to the velocity operator
- Velocity is strongly suppressed near magic angle as the band becomes flat
- The layer counter-flow velocity remain finite.
- The pair potential has opposite signs in the *d* wave channel.

d-wave pairing

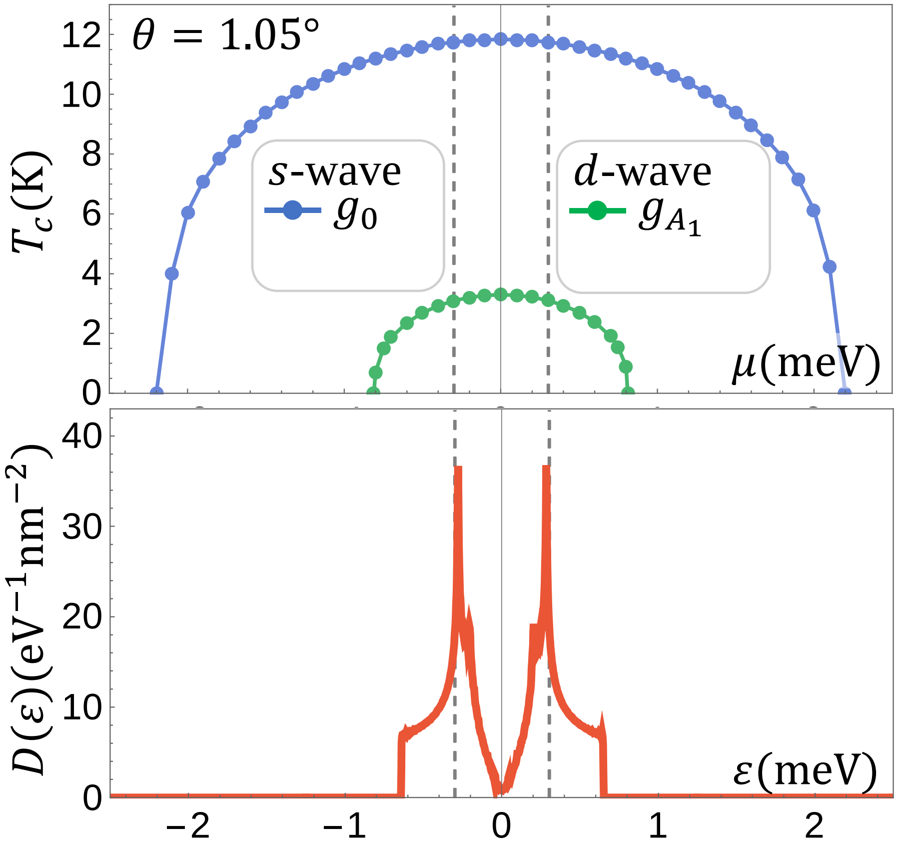

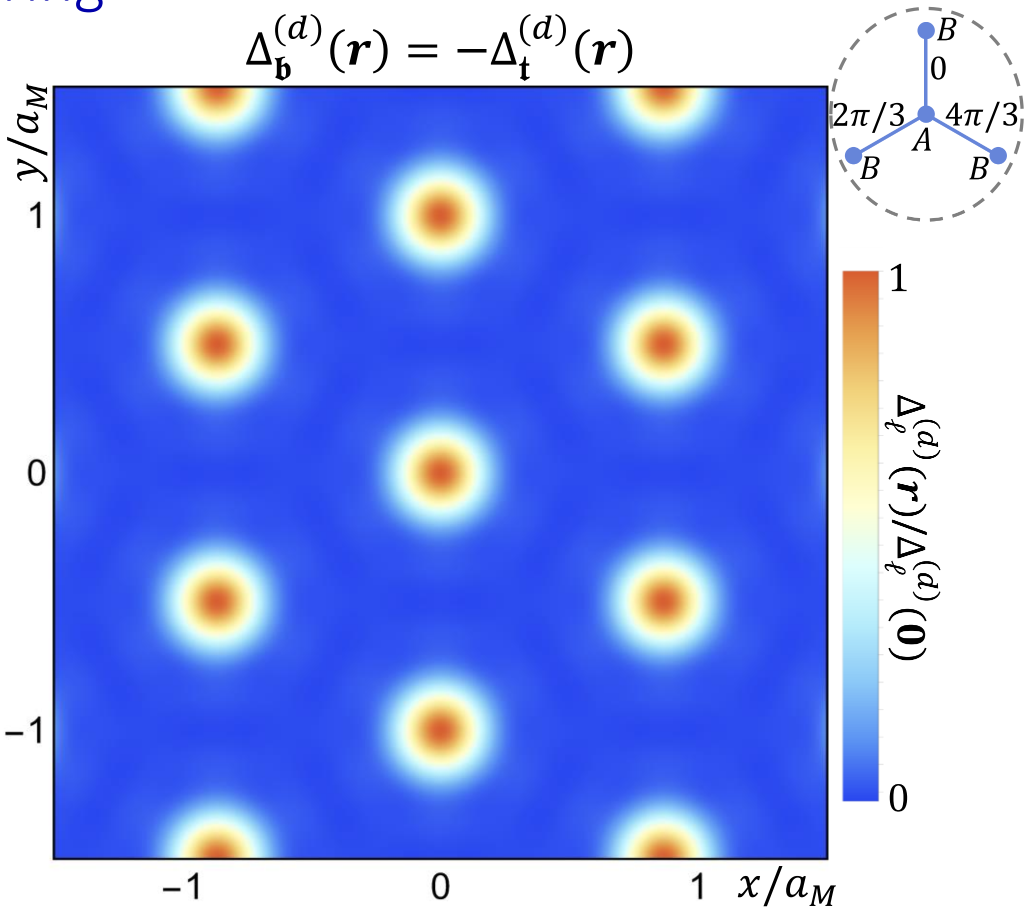

- $T_c \sim 3$ K in d-wave channel. s-wave has a higher T_c.
- The pair potential has spatial modulation as in the s-wave channel .

Coulomb repulsion

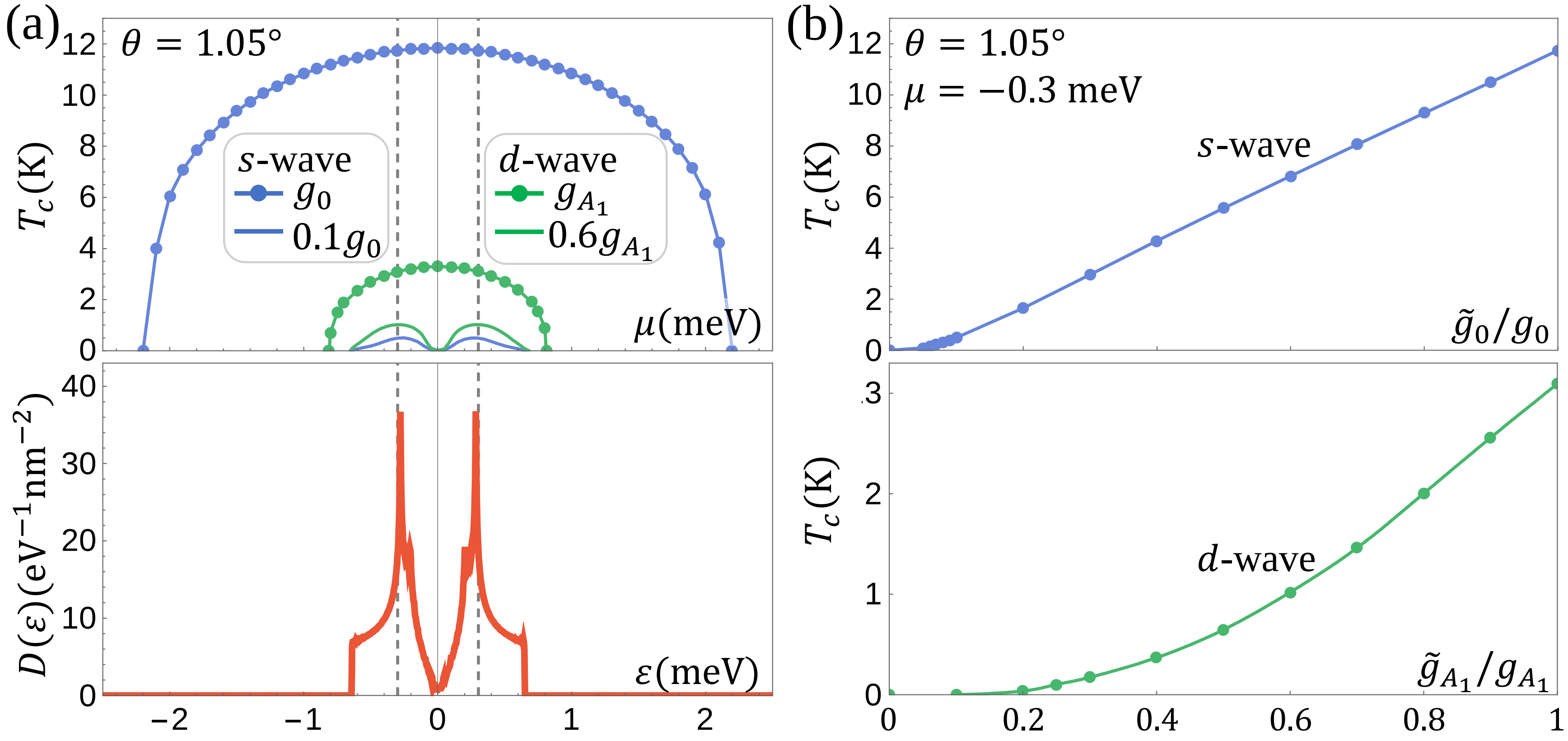

- On-site (U_0) and nearest-neighbor (U_1) respectively suppresses s and d wave pairings.
- If s-wave has $T_c \sim 1.7$ K, $U_0 \approx 3.2$ eV
- If d-wave has $T_c \sim 1.7$ K, $U_1 \approx 0.5$ eV
- Depending on values of U_0 and U_1, either channel can be the leading superconductivity instability
- U_0 can drive correlated insulating states.
- When the attractive interaction is reduced by repulsion, there is a dip in T_c at charge-neutrality point.

Discussion

- Phonons generate attractive interaction in both *s* and *d* wave pairing channels.

- Phonon-mediated attractive interaction combined with local repulsion can provide a model to study competition between superconductivity and correlated insulating states.

- Other phonon modes can further enhance attraction in s-wave channel:
  T. J. Peltonen, R. Ojajärvi, T. T. Heikkilä, PRB (2018)
  B. Lian, Z. Wang, B. A. Bernevig, arXiv:1807.04382
  Y. W. Choi and H. J. Choi, PRB (2018)
  F. Wu, , E. Hwang, S. Das Sarma, arXiv:1811.04920

- Long-range Coulomb preserves SU(2)×SU(2) symmetry ➔d-wave & p-wave are degenerate
  H. Isobe, N. F.Q. Yuan, and L. Fu, PRX (2018); Y.-Z. You, A. Vishwanath, arXiv: 1805.06867

✓ Inter-valley phonons tip balance towards d-wave.

Topological Chiral *d*-wave SC

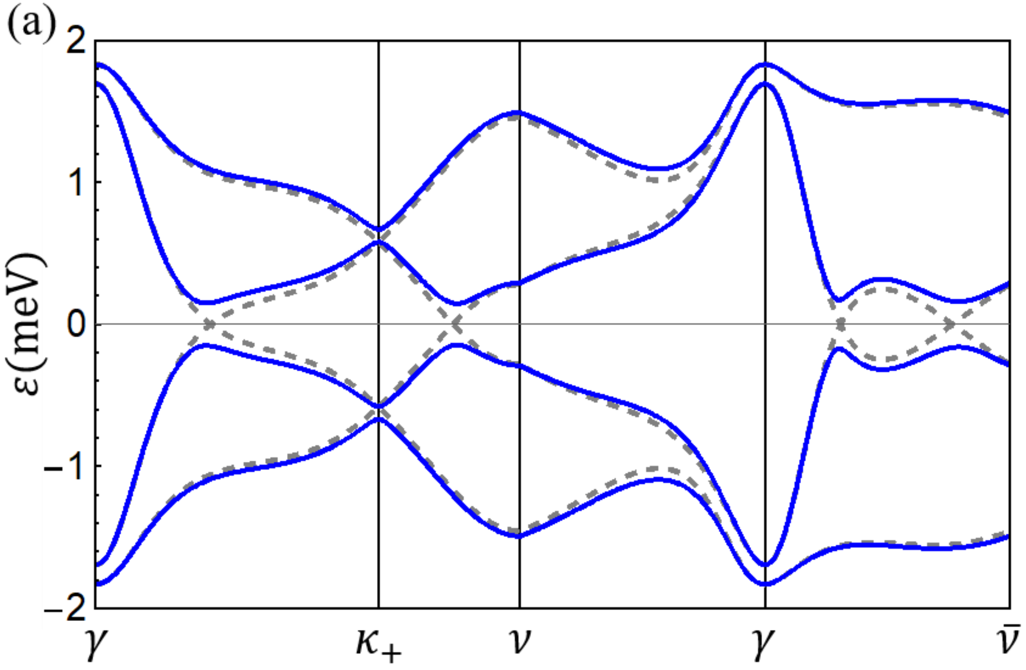

BdG band structure

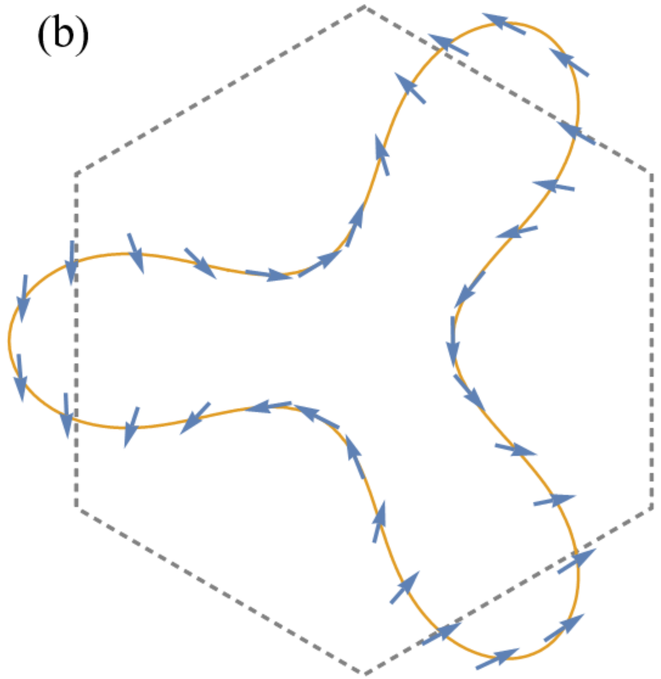

Gap structure

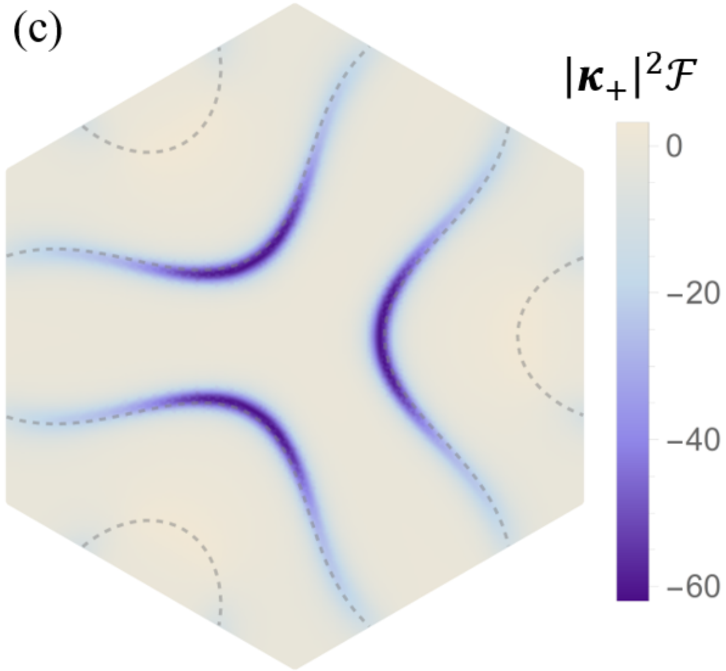

Berry curvature

- Chiral d-wave SC is fully gapped
- Chern number = 4

Spontaneous Vortex-Antivortex

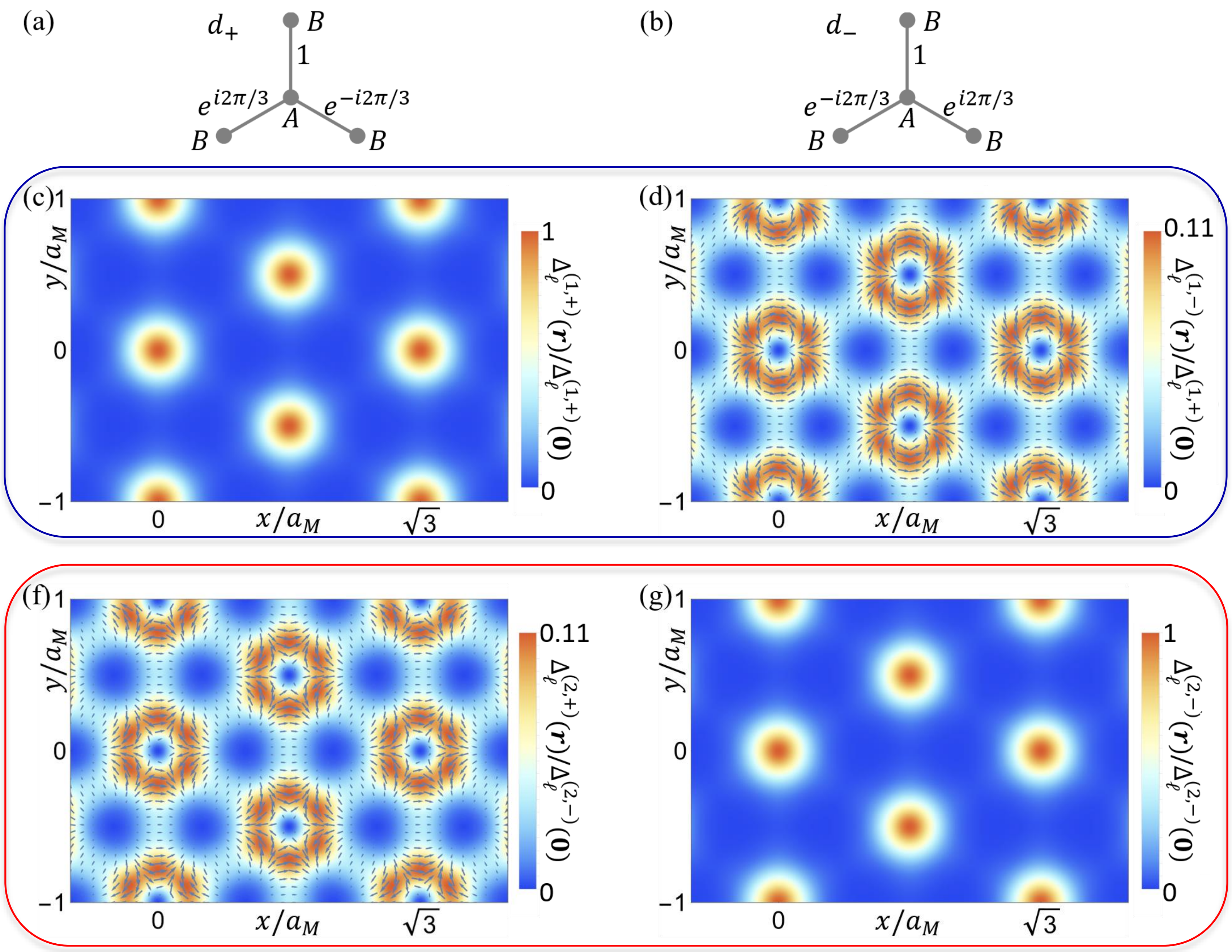

- Cooper pair: 2-*e* bound state
  Relative motion (RM)
  Center-of-mass motion (COMM)
- Angular momentum:
  $L = L_R + L_C$
- $L = +2$
  $(L_R, L_C) = (+2, \quad 0)$
  $(L_R, L_C) = (-2, -2)$
- $L = -2$
  $(L_R, L_C) = (+2, +2)$
  $(L_R, L_C) = (-2, \quad 0)$

Spontaneous Supercurrent

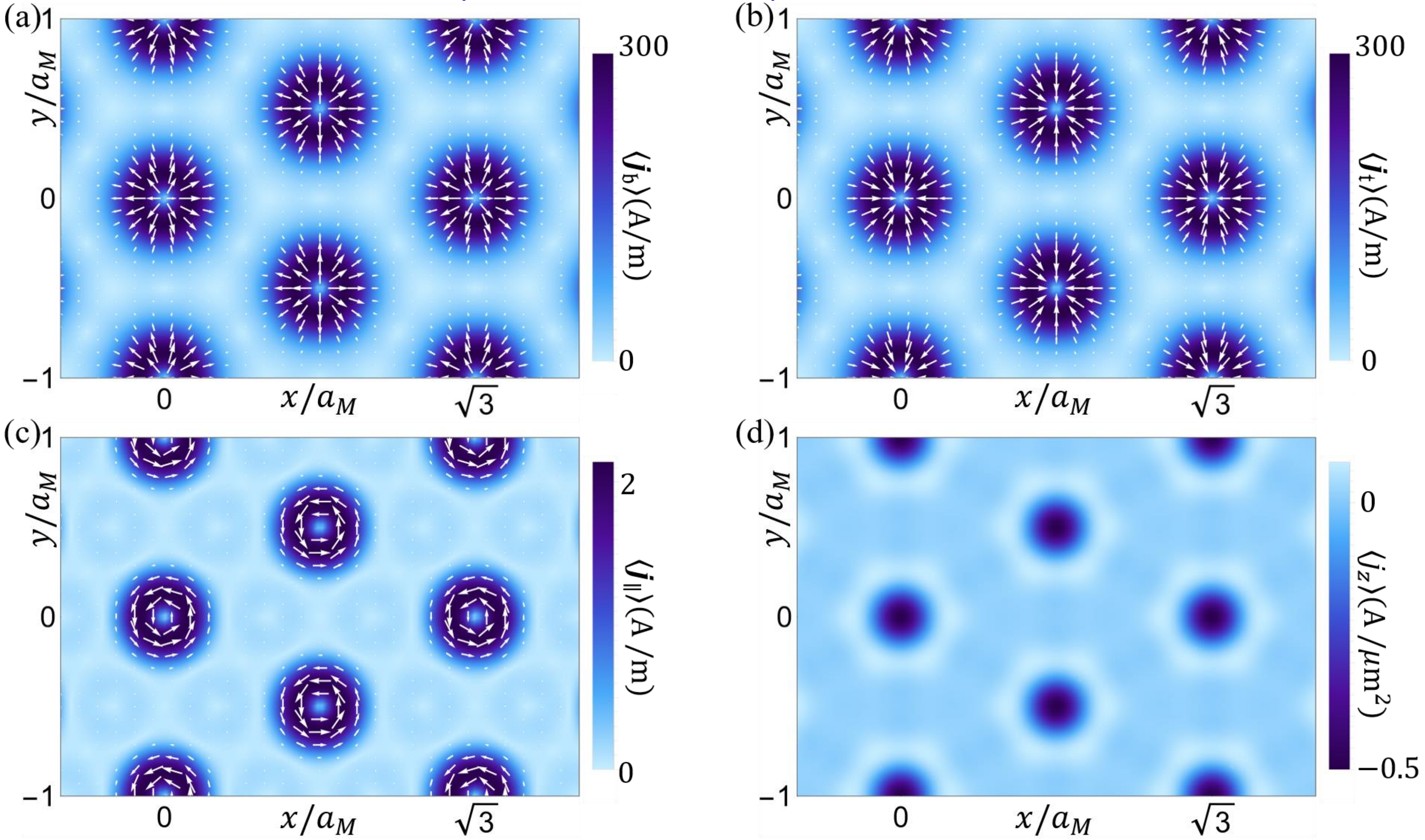

- Each moiré unit cell contains a large number of atomic sites that support current flow.
- Spontaneous supercurrent: magnetic dipole moment & magnetic toroidal dipole moment.

Nematic d-wave SC

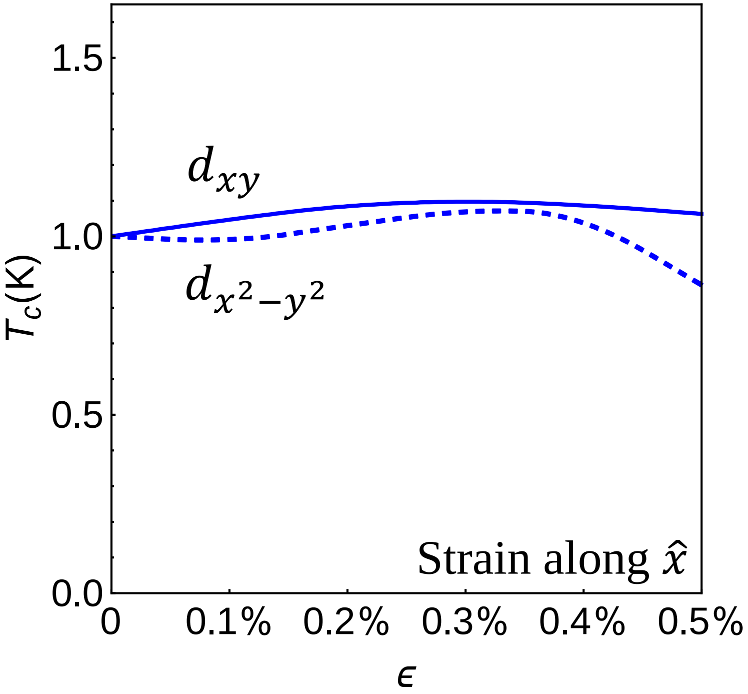

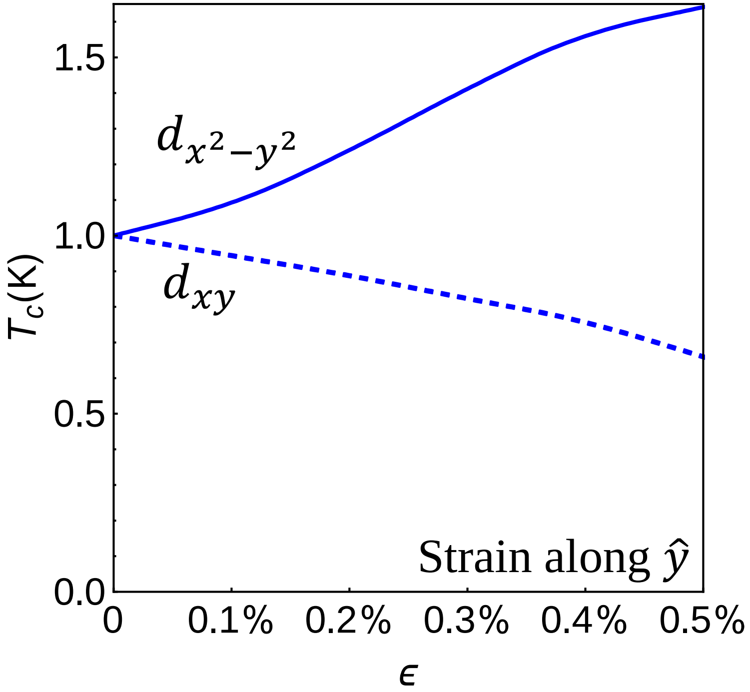

Uniaxial strain stabilizes nematic d-wave

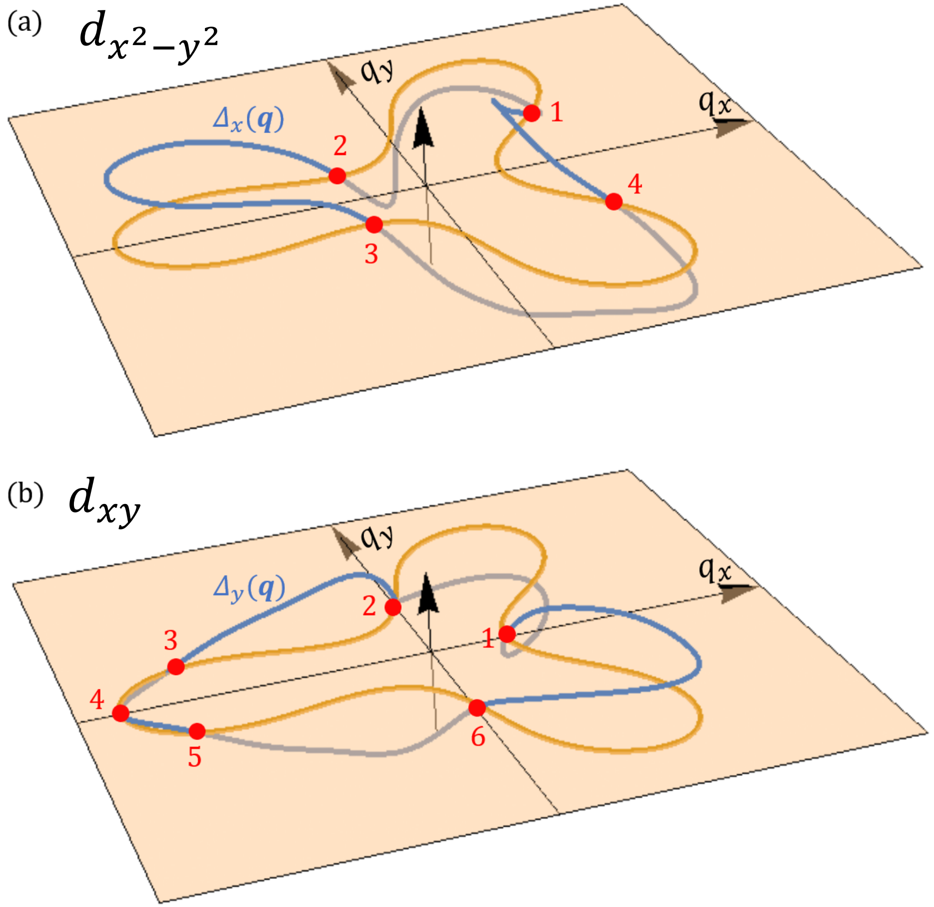

Gap structure with point nodes

$d_{x^2-y^2}$: $\hat{\Gamma}_x = i(\hat{\Gamma}_+ - \hat{\Gamma}_-)/\sqrt{2}$

d_{xy}: $\hat{\Gamma}_y = (\hat{\Gamma}_+ + \hat{\Gamma}_-)/\sqrt{2}$

$\hat{\Gamma}_{\boldsymbol{\eta}} = \eta_x \hat{\Gamma}_x + \eta_y \hat{\Gamma}_y$

$\boldsymbol{\eta} = (\eta_x, \eta_y)$

Nematic order parameter:

$\boldsymbol{N} = (|\eta_x|^2 - |\eta_y|^2, \eta_x^* \eta_y + \eta_y^* \eta_x)$

Critical in-plane magnetic field in *d*-wave channel

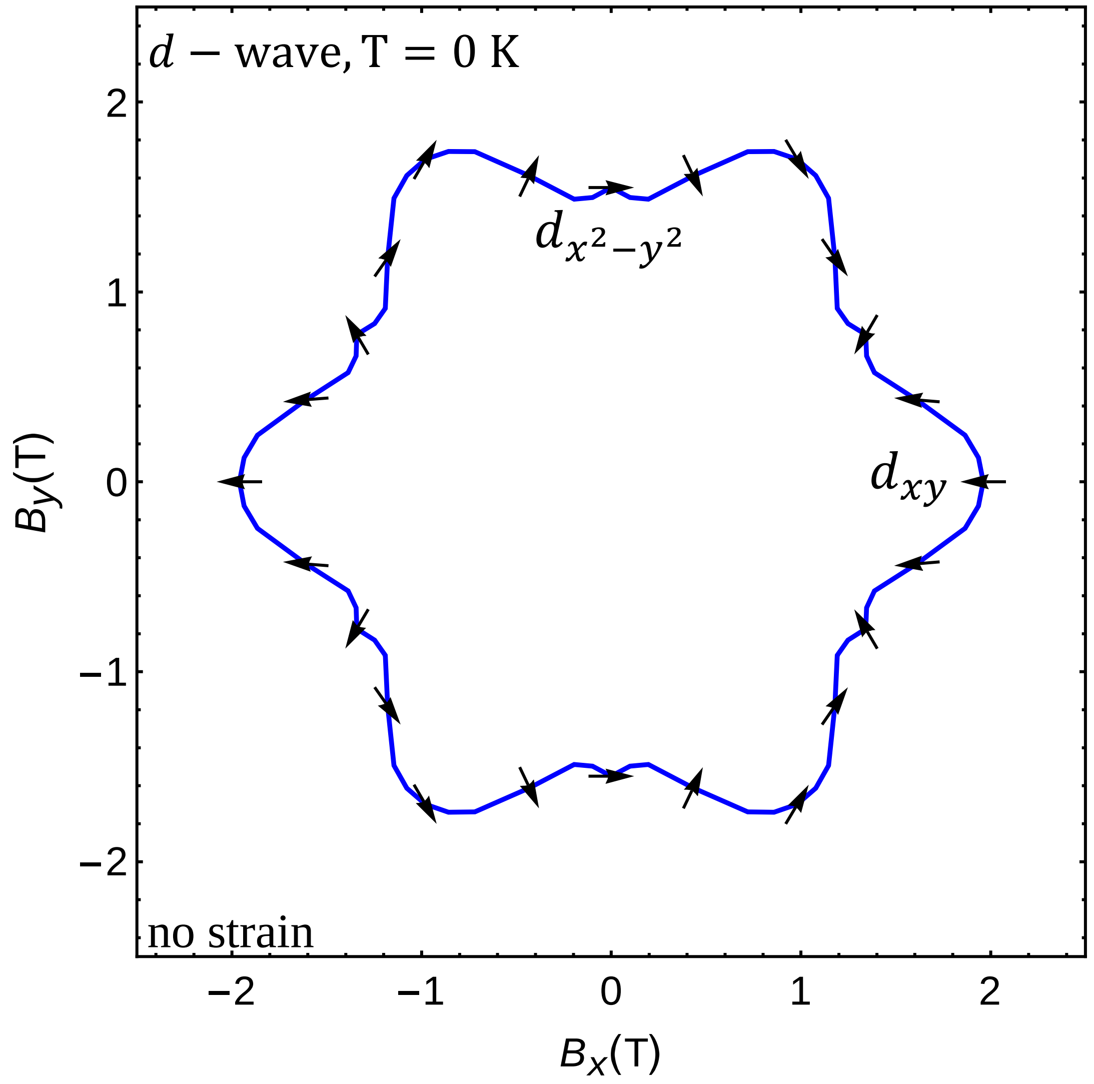

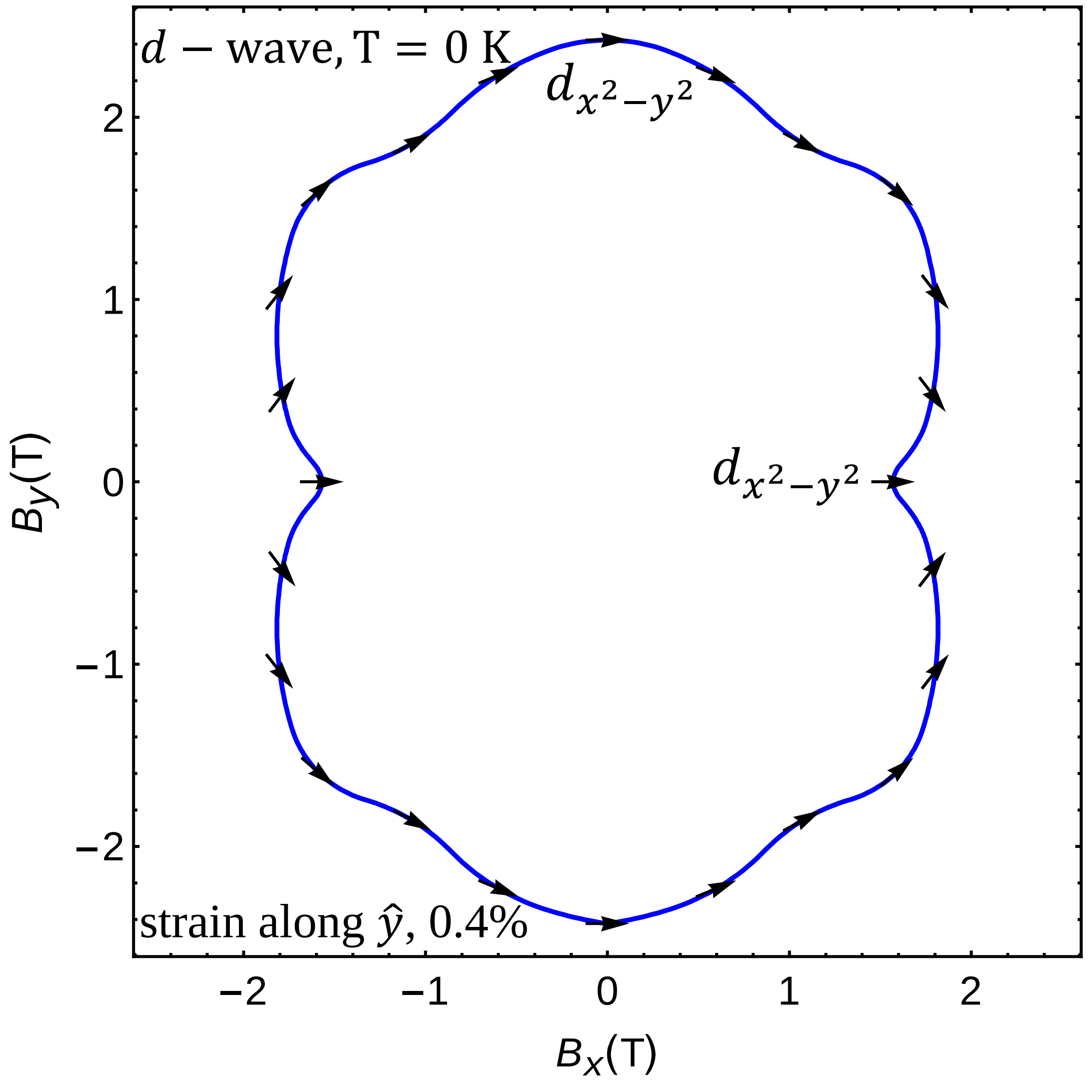

- In-plane magnetic field can also stabilize nematic *d*-wave state.
- Uniaxial strain results in a 2-fold anisotropy of the critical $B_{\parallel}$.

Nematic order parameter:

$$\boldsymbol{N} = (|\eta_x|^2 - |\eta_y|^2, \eta_x^* \eta_y + \eta_y^* \eta_x)$$

s-wave channel

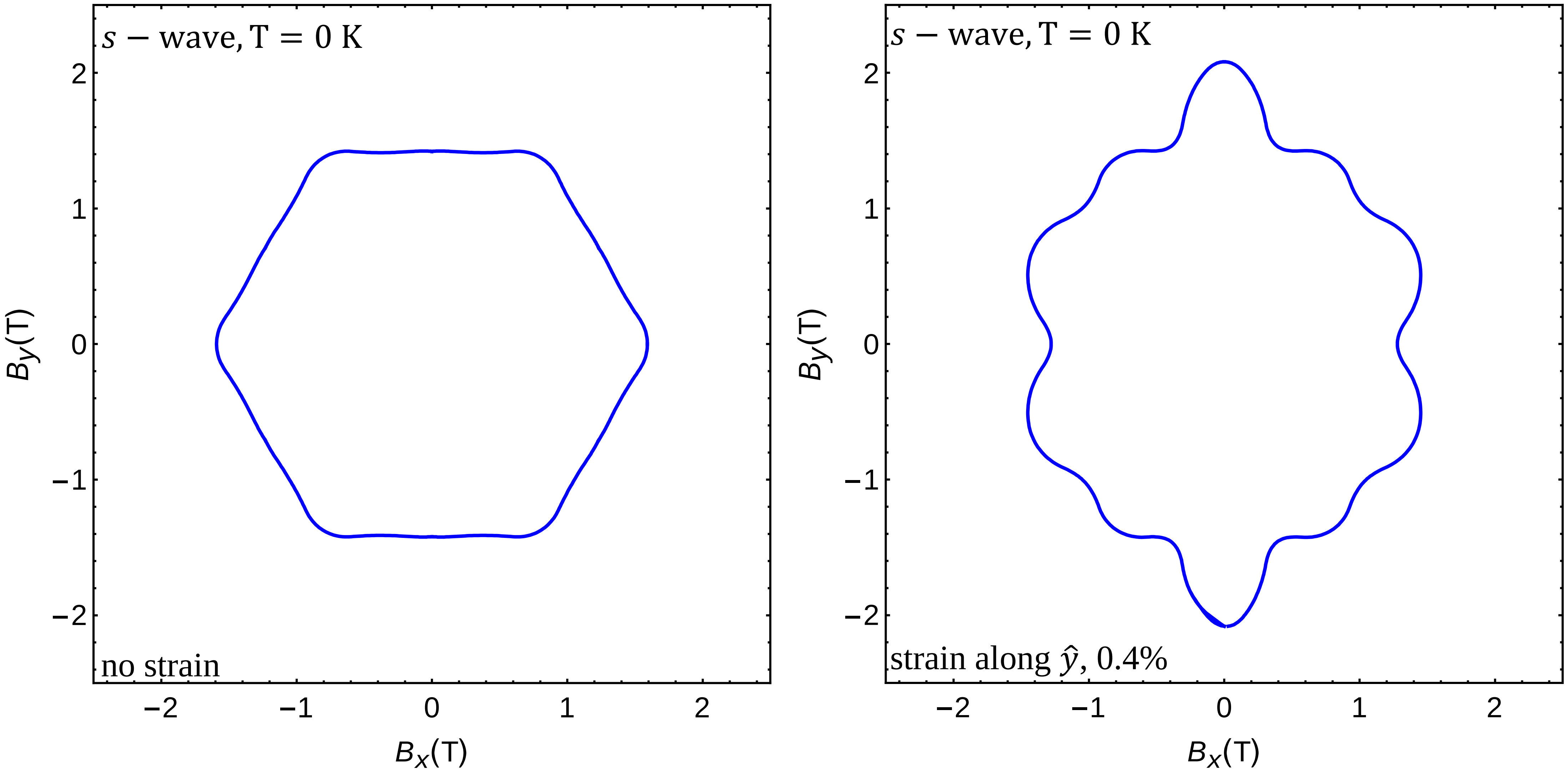

- Uniaxial strain also results in a 2-fold anisotropy of the critical $B_{\parallel}$ in s-wave channel.
- Magic-angle band structure can be sensitive to strain effects.

Summary

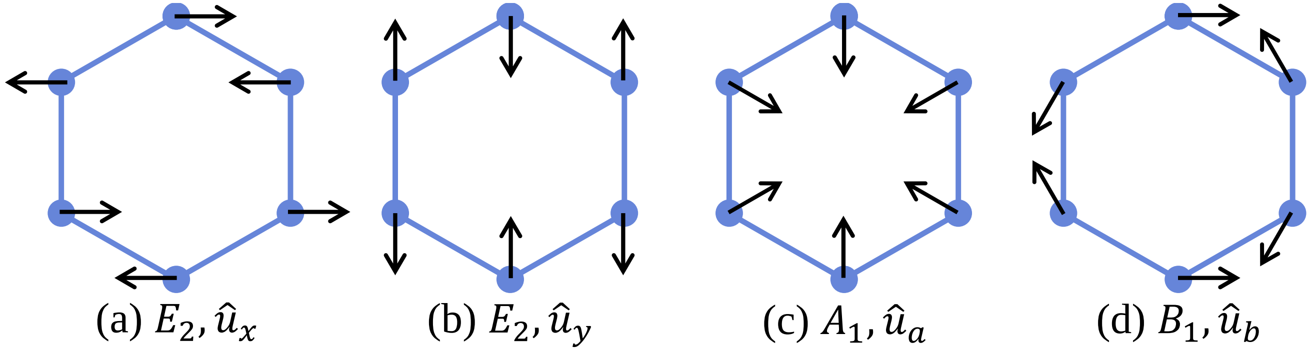

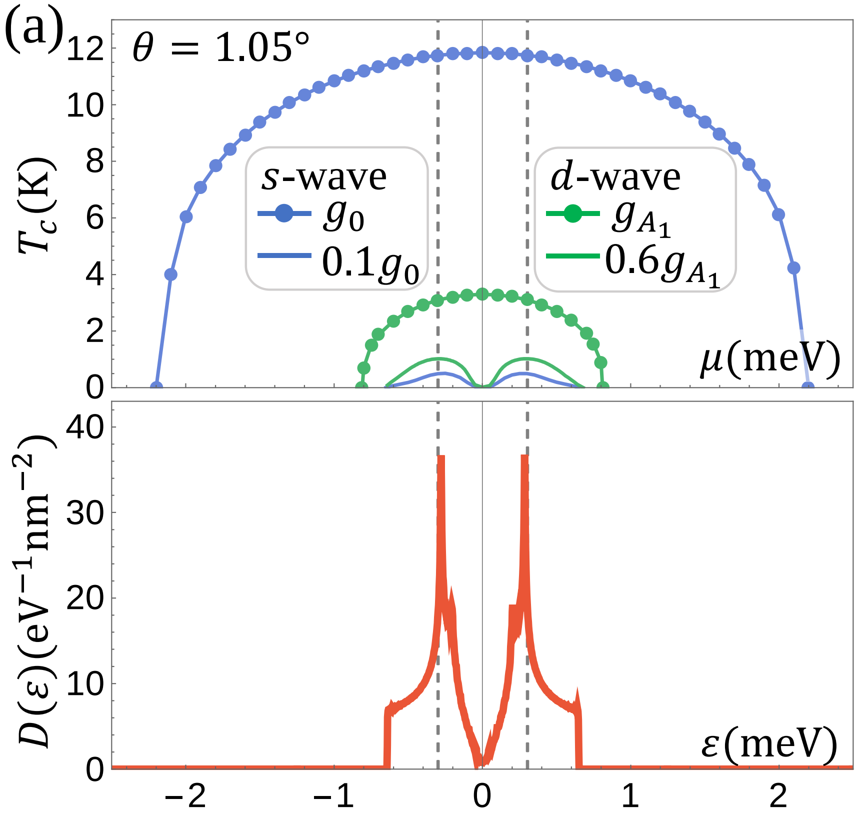

Intervalley optical phonons
Sublattice pseudospin chirality } ⇨ d-wave

Band flattening ⇨ T_c

Thank You!